Wind and Structures, Vol. 16, No. 4 (2013) 323-340
DOI: http://dx.doi.org/10.12989/was.2013.16.4.323

Bridge flutter control using eccentric rotational actuators

R. Körlin * and U. Starossek

Structural Analysis and Steel Structures Institute, Hamburg University of Technology, Denickestr. 17, 21073 Hamburg, Germany

(Received November 5, 2010, Revised March 30, 2012, Accepted May 8, 2012)

Abstract. An active mass damper system for flutter control of bridges is presented. Flutter stability of bridge structures is improved with the help of eccentric rotational actuators (ERA). By using a bridge girder model that moves in two degrees of freedom and is subjected to wind, the equations of motion of the controlled structure equipped with ERA are established. In order to take structural nonlinearities into consideration, flutter analysis is carried out by numerical simulation scheme based on a 4th-order Runge-Kutta algorithm. An example demonstrates the performance and efficiency of the proposed device. In comparison with known active mass dampers for flutter control, the movable eccentric mass damper and the rotational mass damper, the power demand is significantly reduced. This is of advantage for an implementation of the proposed device in real bridge girders. A preliminary design of a realization of ERA in a bridge girder is presented.

Keywords: vibration control; active mass damper; eccentric rotational actuator; bridge; flutter

1. Introduction

Bridge deck flutter is an aeroelastic instability phenomenon. Without advance warning, the self-excited coupled, vertical and torsional vibration may cause collapse. Until now, active flutter control has not yet been implemented in real bridge structures. For reduction of vibration and for prevention of bridge deck flutter, future ultra-long-span bridges may need effective and robust active control devices. Especially, the stabilization of instable erection stages of such bridges could be a main task of the control. The two principal classes of active control measures to avoid flutter vibrations are the aerodynamic measures and the mechanical measures. Both can be used for stabilization through feedback controller.

Active mass dampers (AMDs) change the dynamic properties of the bridge structure and enhance flutter stability, e.g. Miyata *et al.* (1996), Wilde *et al.* (1996). In Körlin and Starossek (2004), AMDs with movable eccentric masses and rotational masses were studied. In these cases, flutter control is carried out using a control moment due to the weight of the eccentric mass or the changing rotational speed of the damper mass, respectively, in order to reduce torsional vibrations of the bridge girder. An alternative flutter control by semi-active or active controllers is proposed in Hwang *et al.* (2008) using vertical dampers installed between the pylon legs and the continuous bridge deck. Active aerodynamic control modify the flow around the bridge deck or generate

*Corresponding author, Dr., E-mail: r.koerlin@tuhh.de

stabilizing aerodynamic forces, e.g., Kobayashi and Nagaoka (1992), Ostenfeld and Larsen (1992). Active aerodynamic countermeasures continue to be studied (e.g., Wilde *et al*. 2001, Phan and Kobayshi 2011). The movable surfaces of aerodynamic control change the appearance of the bridge. A merit is the generation of damping forces using the energy of the wind flow. In contrast, mechanical devices use only external energy from a power supply. However, they can be installed completely inside the bridge deck. There are some implementations of active mechanical control for vibrations of high rise buildings and bridge pylons induced by earthquakes (Spencer Jr. and Sain 1997). Therefore, the active mechanical control is in the focus of authors' research. Results of a wind tunnel experiment in Körlin and Starossek (2007) underline the applicability of an active mass damper.

In this paper, a rotational actuator system for flutter suppression with two eccentric rotational actuators (ERA) is proposed. A two-dimensional sectional model has been used to describe the structural dynamics of a bridge deck subjected to wind. The motion-induced aerodynamic forces are considered in the analysis using frequency-dependent flutter derivatives that have been obtained experimentally. The flutter analysis of the uncontrolled and controlled structure has been carried out using suitable rational function approximations (RFA) of the unsteady aerodynamic forces (Karpel and Strul 1996, Tiffany and Adams Jr. 1987). Because of nonlinearities in the AMD system, critical wind speeds of the controlled structure are determined for different vibration levels using a numerical simulation scheme in the time domain. Several control scenarios have been simulated.

In bridge engineering, one barrier for implementing AMDs seems to be the energy demand. Therefore, in a first step, the energy consumption of the proposed device is investigated and compared to the energy demand of known AMDs. In future research, proving the technical advantages of ERA in comparison to other devices, the robustness due to uncertainties in the parameters of the motion induced aeroelastic forces has to be investigated. Especially, the comparison to the passive and semi active devices, the tuned mass damper (e.g., Kwon and Park 2003), the semi active mass damper (e.g., Abdel-Rohman and Joseph 2006, Gu 2007), and the multiple tuned mass damper (e.g., Ubertini 2010) will be of high interest. In this paper, finally, a preliminary design of the ERA mass damper is presented to give an idea of practical realization of the proposed damper.

2. Flutter control with eccentric rotational actuators (ERA)

2.1 Proposed active mass damper

The bridge girder moves in two degrees of freedom, the vertical displacement h and the rotational displacement α. The transverse displacement is not considered here. The proposed AMD consists of a pair of eccentric rotational actuators (ERA), Fig. 1. The rotational movements γ_1 and γ_2 of the rotating arms are in relation to horizontal position.

The following quantities are introduced: the mass inertias of bridge girder m and I, the two additional control masses m_c, the damping ratios c_h and c_α, the spring constants k_h and k_α, the control forces M_{c1} and M_{c2}, as well as the aerodynamic forces A (lift) and M (pitching moment). The introduced system parameters and aerodynamic forces are quantities per unit length. The length of a rotating arm is e_c. The eccentricity of the rotating mass dampers is b_c, and b is half the width of the bridge deck.

With the help of suitable actuators, e.g. hydraulic or electric actuators, the rotating arms carry out controlled angular movements which depend on measured bridge vibrations. For the time being, there are no restrictions on whether angular movements are allowed only up to certain amplitudes around zero state, or whether the control masses can move along the whole circumference of the circle around the respective axis of rotation.

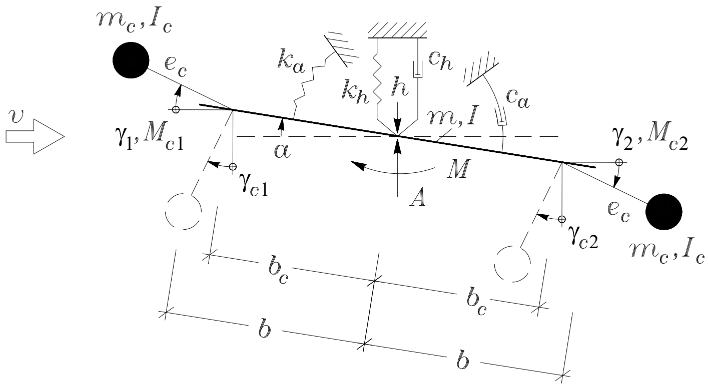

Fig. 1 Damper with eccentric rotational actuators (ERA)

2.2 Equations of motion

In this section, we first take a look at the system with the rotating arms resting in a vertical position (due to gravitation), with no influence of actuators. In order to deduce the equation of motion, it is convenient to introduce the auxiliary quantities γ_{c1} and γ_{c2} as rotational movements of the rotating arms, see Fig. 1

$$\gamma_{c1} = \gamma_1 - \frac{\pi}{2}, \quad \gamma_{c2} = \gamma_2 + \frac{\pi}{2} \tag{1}$$

The kinetic energy E_k can be deduced with the help of the coordinates x_1, x_2, y_1 and y_2

$$E_k = \frac{1}{2}m\dot{h}^2 + \frac{1}{2}m_c(\dot{x}_1^2 + \dot{y}_1^2 + \dot{x}_2^2 + \dot{y}_2^2) + \frac{1}{2}I_c(\dot{\gamma}_{c1}^2 + \dot{\gamma}_{c2}^2) + \frac{1}{2}I\dot{\alpha}^2 \tag{2}$$

where $x_1 := -e_c \sin\gamma_{c1} - b_c \cos\alpha$
$x_2 := -e_c \sin\gamma_{c2} + b_c \cos\alpha$
$y_1 := -e_c \cos\gamma_{c1} + b_c \sin\alpha - h$
$y_2 := -e_c \cos\gamma_{c2} - b_c \sin\alpha - h$.

The potential energy E_p is quantified as follows

$$E_p = \frac{1}{2}k_h h^2 + \frac{1}{2}k_\alpha \alpha^2 - (m + 2m_c)gh + m_c g e_c[(1 - \cos\gamma_{c1}) + (1 - \cos\gamma_{c2})] \tag{3}$$

where g is the constant of gravitation. For the dynamics of the structure, it is not necessary to consider the potential energy due to the gravitation in h. The term $(m + 2m_c)gh$ is neglected. The function of Lagrange L can be established

$$L \equiv E_k - E_p \tag{4}$$

Evaluating this expression gives

$$\begin{gathered} L = \frac{1}{2}(m + 2m_c)\dot{h}^2 + \frac{1}{2}(I + 2m_c b_c^2)\,\dot{\alpha}^2 + \dots \\ + \frac{1}{2}(I_c + m_c e_c^2)(\dot{\gamma}_{c1}^2 + \dot{\gamma}_{c2}^2) + m_c g e_c(\cos\gamma_{c1} + \cos\gamma_{c2}) + \dots \\ - m_c e_c \dot{h}(\dot{\gamma}_{c1}\sin\gamma_{c1} + \dot{\gamma}_{c2}\sin\gamma_{c2}) - \frac{1}{2}k_h h^2 + \dots \\ + m_c e_c b_c \dot{\alpha}[\dot{\gamma}_{c1}\sin(\gamma_{c1} - \alpha) - \dot{\gamma}_{c2}\sin(\gamma_{c2} - \alpha)] - \frac{1}{2}k_\alpha \alpha^2 \end{gathered} \tag{5}$$

where in this representation the potential energy is shifted by a constant amount. This fact has no further influence on the equations of motion, since they contain only derivations of L.

With regard to the four generalized coordinates of interest, the system of equations of motion contains the following four Euler-Lagrange equations

$$\begin{gathered} \frac{\mathrm{d}}{\mathrm{d}t}\left(\frac{\partial L}{\partial \dot{h}}\right) - \frac{\partial L}{\partial h} = -A - c_h \dot{h} \\ \frac{\mathrm{d}}{\mathrm{d}t}\left(\frac{\partial L}{\partial \dot{\alpha}}\right) - \frac{\partial L}{\partial \alpha} = M - (M_{c1} + M_{c2}) - c_\alpha \dot{\alpha} \\ \frac{\mathrm{d}}{\mathrm{d}t}\left(\frac{\partial L}{\partial \dot{\gamma}_{c1}}\right) - \frac{\partial L}{\partial \gamma_{c1}} = M_{c1} \\ \frac{\mathrm{d}}{\mathrm{d}t}\left(\frac{\partial L}{\partial \dot{\gamma}_{c2}}\right) - \frac{\partial L}{\partial \gamma_{c2}} = M_{c2} \end{gathered} \tag{6}$$

The terms of the equations of motion are not presented here for sake of brevity. Since they are of more interest regarding vibration damping of main bridge girders, the system equations with the angles γ_1 and γ_2 will be presented here; cf. Eq. (1). In order for both rotating arms to shift into the new, horizontal equilibrium positions (zero positions), control forces are needed. Furthermore, the masses of the rotating arms need to be permanently compensated

$$M_{c1} = M_1 + m_c e_c g \cos\gamma_1 \,, \quad M_{c2} = M_2 - m_c e_c g \cos\gamma_2 \tag{7}$$

The control forces M_1 and M_2 are used to control the active mass damper ERA, whereas the remaining terms of the states γ_1 and γ_2 are a nonlinear compensation of the gravitational effects.

After inserting the respective quantities into the equations, the nonlinear system of differential equations reads

$$\begin{gathered}(m + 2m_c)\ddot{h} + c_h\dot{h} + k_h = -A + \;\ldots \\ +m_c e_c(\ddot{\gamma}_1 \cos\gamma_1 - \dot{\gamma}_1^2 \sin\gamma_1 + \dot{\gamma}_2^2 \sin\gamma_2 - \ddot{\gamma}_2 \cos\gamma_2)\end{gathered} \tag{8}$$

$$\begin{gathered}(I + 2m_c b_c^2)\ddot{\alpha} + c_\alpha\dot{\alpha} + k_\alpha\alpha = M - (M_1 + M_2) + \;\ldots \\ +m_c e_c b_c[\dot{\gamma}_1^2 \sin(\gamma_1 - \alpha) - \ddot{\gamma}_1 \cos(\gamma_1 - \alpha)\,] + \;\ldots \\ +m_c e_c b_c[\dot{\gamma}_2^2 \sin(\gamma_2 - \alpha) - \ddot{\gamma}_2 \cos(\gamma_2 - \alpha)\,]\end{gathered} \tag{9}$$

$$\begin{gathered}(I_c + m_c e_c^2)\ddot{\gamma}_1 = M_1 + m_c e_c\ddot{h} \cos\gamma_1 - \;\ldots \\ -m_c e_c b_c[\dot{\alpha}^2 \sin(\gamma_1 - \alpha) + \ddot{\alpha} \cos(\gamma_1 - \alpha)]\end{gathered} \tag{10}$$

$$\begin{gathered}(I_c + m_c e_c^2)\ddot{\gamma}_2 = M_2 - m_c e_c\ddot{h} \cos\gamma_2 - \;\ldots \\ -m_c e_c b_c[\dot{\alpha}^2 \sin(\gamma_2 - \alpha) + \ddot{\alpha} \cos(\gamma_2 - \alpha)]\end{gathered} \tag{11}$$

According to these equations, the structure is not influenced by gravitation any more.

2.3 Control algorithm

The closed loop needs to be stable and has to show a good decay behavior with respect to occurring disturbances. For the time being, it shall not be stated here whether it is necessary to demand either local stability in a limited surrounding of an equilibrium point or global stability in the entire state space.

The transverse displacement of the main bridge girder is neglected here. In order to be able to exclude horizontal inertia forces of the ERA damper, both rotating arms are synchronized or counter-rotating –the magnitudes of γ_1 and γ_2 have to correspond with each other within the scope of a control scenario at any given time. The control effort should be reasonable, e.g., the vibration control should have a moderate energy demand. A limiting maximum control force is not to be exceeded.

For active damping, the centrifugal forces of the rotating eccentric masses can be used cf. Starossek and Scheller (2008). Depending on the frequency of motion of the bridge girder, the control determines the angular velocities, $\dot{\gamma}_1$ and $\dot{\gamma}_2$. Alternatively, active damping can be applied generating inertia forces in vertical direction due to the acceleration of the eccentric arms nearby the horizontal equilibrium positions. Now, there are two control tasks in order to achieve the control objectives: The first task concerns the positioning of rotating arms – position control –, and the second task relates to the active damping of bridge vibrations – dynamic control. Both controls may interfere with each other. If the dynamic control generates a torque in the actuators, the rotating arms are driven out of their equilibrium point. The position control will then immediately try to move the rotating arms back to equilibrium point. This will curtail the dynamic control action. If the action of the position control is too strong, the effect of the dynamic control will be lost and vice versa.

On account of the nonlinearities in the ERA system, the application of nonlinear controls is quite reasonable and necessary in order to achieve a satisfying control performance. In this case, in order to solve the problem and to apply the respective methods to ERA, it is beneficial to use the affinity of the control-related problem on hand to the benchmark problem known in control engineering, namely the translational oscillator with the rotational actuator (TORA), cf. in Bupp *et al.* (1995).

Control objectives may be achieved using the following control laws, cf. Körlin *et al.* (2011),

$$M_1(t) = \frac{k_\alpha(I_c + m_c e_c^2)}{2(I + 2m_c b_c^2)}[(1+\cos\gamma_1)\mathbf{K}_1 + (1-\cos\gamma_1)\mathbf{K}_2]\begin{pmatrix}\beta_c\alpha \\ \beta_c\tau\dot{\alpha} \\ \gamma_1 \\ \tau\dot{\gamma}_1\end{pmatrix}$$

$$M_2(t) = \frac{k_\alpha(I_c + m_c e_c^2)}{2(I + 2m_c b_c^2)}[(1+\cos\gamma_2)\mathbf{K}_1 + (1-\cos\gamma_2)\mathbf{K}_2]\begin{pmatrix}\beta_c\alpha \\ \beta_c\tau\dot{\alpha} \\ \gamma_2 \\ \tau\dot{\gamma}_2\end{pmatrix} \tag{12}$$

with

$$\beta_c := \sqrt{\frac{(I + 2m_c b_c^2)}{2(I_c + m_c e_c^2)}}\,, \quad \tau := \sqrt{I + \frac{2m_c b_c^2}{k_\alpha}}$$

The 1×4-matrices $\mathbf{K}_1$ and $\mathbf{K}_2$ are the control matrices and contain 4 control parameters each. The measured state quantities α, $\dot{\alpha}$, γ_1, γ_2, $\dot{\gamma}_1$ and $\dot{\gamma}_2$ determines the control forces M_1 and M_2. For sake of brevity, the details of the derivation of the control law are not presented here and can be found in Körlin *et al.* (2011).

3. Flutter analysis

3.1 Aerodynamic forces

The aerodynamic forces on the bridge deck consist of motion-induced aerodynamic forces, the aeroelastic forces A_L and M_L, and of the motion-independent aerodynamic forces A_B and M_B which result from gust or turbulence in the oncoming flow. In linear theory, the following superposition is valid

$$A = A_L + A_B\,, \quad M = M_L + M_B \tag{13}$$

Following the complex number approach in Starossek (1998), the motion-induced aerodynamic forces can be expressed in the following linearized form if a constant-amplitude sinusoidal structural motion is assumed

$$\mathbf{F} = \begin{pmatrix} -A_L b \\ M_L \end{pmatrix} = \pi \rho \upsilon^2 b^2 \mathbf{Q}\mathbf{x} \tag{14}$$

with

$$\mathbf{Q} := k^2 \begin{pmatrix} c_{hh}(k) & c_{h\alpha}(k) \\ c_{\alpha h}(k) & c_{\alpha\alpha}(k) \end{pmatrix}, \quad \mathbf{x} := \begin{pmatrix} h/b \\ \alpha \end{pmatrix}$$

where υ is the mean velocity of the oncoming flow and ρ is the air density. The non-dimensional reduced frequency k is defined as $k = \omega b/\upsilon$, where ω is the circular frequency of structural motion. The $c_{mn} = c'_{mn} + ic''_{mn}$ with m, n = h, α are dimensionless complex flutter derivatives, where c'_{mn} and c''_{mn} are real numbers and i is the imaginary unit. The complex flutter derivatives are functions of the reduced frequency k and depend on the cross section under consideration.

Alternatively, following the real notation approach by Scanlan in its latest form (Simiu and Scanlan 2008), the aeroelastic forces can be expressed as

$$\begin{aligned} -A_L &= \frac{1}{2}\rho \upsilon^2 B \left[K H_1^*(K)\frac{\dot{h}}{\upsilon} + K H_2^*(K)\frac{B\dot{\alpha}}{\upsilon} + K^2 H_3^*(K)\alpha + K^2 H_4^*(K)\frac{h}{B} \right] \\ M_L &= \frac{1}{2}\rho \upsilon^2 B^2 \left[K A_1^*(K)\frac{\dot{h}}{\upsilon} + K A_2^*(K)\frac{B\dot{\alpha}}{\upsilon} + K^2 A_3^*(K)\alpha + K^2 A_4^*(K)\frac{h}{B} \right] \end{aligned} \tag{15}$$

where K is defined as $K = B\omega/\upsilon$ and B is the width of the bridge deck. The eight real coefficients H_j^* and A_j^* (j = 1, ..., 4) are the flutter derivatives based on this notation. The relationship between these two formulations is as follows

$$c'_{hh} = \frac{2}{\pi}H_4^*\,, \quad c''_{hh} = \frac{2}{\pi}H_1^*\,, \quad c'_{\alpha h} = \frac{4}{\pi}A_4^*\,, \quad c''_{\alpha h} = \frac{4}{\pi}A_1^* \tag{16}$$

$$c'_{h\alpha} = \frac{4}{\pi} H_3^*\,, \quad c''_{h\alpha} = \frac{4}{\pi} H_2^*\,, \quad c'_{\alpha\alpha} = \frac{8}{\pi} A_3^*\,, \quad c''_{\alpha\alpha} = \frac{8}{\pi} A_2^* \tag{17}$$

In Starossek (1998) both methods of analysis are compared. Complex notation provides a more compact and natural representation of the aerodynamic forces and of the ensuing eigenvalue problem. Another advantage of the notation used here is that the particular meaning of each derivative follows from its indices.

Regarding the rational function approximation (RFA) of the unsteady aeroelastic forces, the minimum state formulation of Karpel and Strul (1996) is used

$$\mathbf{Q}(k) \simeq \mathbf{A}_0 + ik\mathbf{A}_1 + (ik)^2\mathbf{A}_2 + \mathbf{D}(ik\mathbf{I} + \mathbf{R})^{-1}\mathbf{E}ik \tag{18}$$

The coefficients of the 2×2-matrices $\mathbf{A}_0$, $\mathbf{A}_1$, $\mathbf{A}_2$ of the 2×N-matrix $\mathbf{D}$ and of the N×2-matrix $\mathbf{E}$ are determined in a linear iterative least-square optimization method, and the N lag terms in the diagonal matrix $\mathbf{R}$ are selected by a nonlinear non-gradient optimizer (Tiffany and Adams Jr. 1987). With the help of the optimization procedure, elements of the matrices are selected, so that the RFA (Eq. (18)) fits the frequency-dependent flutter derivatives (Eq. (14)). The transformation into the time domain reads

$$\mathbf{Q}\,\mathbf{x} = \mathbf{A}_0\mathbf{x} + \frac{b}{v}\mathbf{A}_1\dot{\mathbf{x}} + \frac{b^2}{v^2}\mathbf{A}_2\ddot{\mathbf{x}} + \mathbf{D}\mathbf{x}_{ae} \tag{19}$$

$$\dot{\mathbf{x}}_{ae} = -\frac{v}{b}\mathbf{R}\mathbf{x}_{ae} + \mathbf{E}\dot{\mathbf{x}} \tag{20}$$

The N aerodynamic lag terms in $\mathbf{x}_{ae}$ model the wind force dynamics acting on the bridge deck.

The motion-independent aerodynamic forces are considered in the quasi-steady form as given in Simiu and Scanlan (2008). In this study, however, only the variation of the horizontal wind speed $v(t)$ is taken into account

$$\mathbf{F}_B = \begin{pmatrix} -A_B b \\ M_B \end{pmatrix} = \pi\rho v^2 b^2 \begin{pmatrix} -2C_L(\alpha) \\ 4C_M(\alpha) \end{pmatrix} \frac{v(t)}{v} \tag{21}$$

The $C_L(\alpha)$ and $C_M(\alpha)$ are the steady aerodynamic coefficients for vertical and rotational mode, respectively.

For the generation of time series of the zero-mean stochastic turbulent component of the wind speed $v(t)$, a Davenport-spectrum $S_v(f)$ with a characteristic length of 1200 m was used (Davenport 1962), where f is the frequency variable. Following the method of Shinozuka and Jan (1972), $v(t)$ can be determined from

$$v(t) = \sum_{l=1}^{n} \sqrt{2S_v(f_l)\Delta f_l} \cos(2\pi f_l t + \varphi_l) \tag{22}$$

a superposition of several cosine functions in the frequency band of interest of the spectrum S_v which is separated into proportional intervals Δf_l with the mean value f_l. The phase angles φ_l are chosen randomly. The turbulence intensity Tu of the generated time series is defined as follows

$$Tu = \frac{\sigma_v}{v} \tag{23}$$

where σ_v is the standard deviation of the time series of wind velocities.

3.2 Numerical simulation of structural response

Applying Eqs. (13), (14), (19) – (21), the equations of motion of the bridge structure equipped with ERA subjected to aerodynamic forces follow from Eqs. (8) – (11). Note that the system is extended by the N equations in Eq. (20). In order to simulate control scenarios, it is necessary to decouple the coupled equations of motion and to solve them using time-step integration. All nonlinear terms as well as other terms which couple equations of motion among each other are to be placed on the right sides of the equations and to be calculated within one time step from the states of the previous time step. The turbulence-induced aerodynamic forces in Eq. (21) are deduced in each time step from the current value of $v(t)$. The classical 4th-order Runge-Kutta formula has been used for numerical integration.

3.3 Flutter condition of nonlinear structures

Flutter calculation is generally carried out in respect to linear or linearized systems with corresponding linear equations of motion under the condition of a smooth oncoming flow (Starossek 1998, Simiu and Scanlan 2008). Nonlinear dependencies are linearized at operating points. Such a procedure is justified only if the states under consideration stay within a sufficiently small operating range where the linear equations of motion are valid. Using the linearized equations of motion and the motion-induced aerodynamic forces from Eq. (14), the determination of critical wind speed can be conducted by a complex eigenvalue analysis (Starossek 1998).

Simulations carried out with respect to the ERA damper show that limitation to small-scale movement of the rotating arms is not possible. Due to the nonlinearities in the ERA system, the definition of flutter stability of controlled structure by a general, amplitude-independent critical wind speed does not suffice. Although not yet established in the field of bridge aerodynamics, several approaches might be possible regarding state-dependent or amplitude-dependent definitions of flutter stability. Standard deviations of displacements could be limited, cf. Körlin *et al.* (2004).

Alternatively, it is suggested to carry out free vibrations tests under the condition of a smooth oncoming flow as a basis for evaluating flutter stability. Using the proposed numerical simulation method, the unstable response of the nonlinear structure could be identified through incremental enhancement of wind speed and subsequent evaluation of phase portraits. If limit cycles are formed in phase portraits, the stability border, i.e., critical wind speed, is found. Because of the nonlinearities in the controlled structure, this stability border depends on the initial displacement $\mathbf{x}_0 = \mathbf{x}(t_0)$ and $\dot{\mathbf{x}}_0 = \dot{\mathbf{x}}(t_0)$ at time $t_0 = 0$.

The proposed numerical simulation or the numerical-experimental simulation scheme described in Körlin *et al.* (2004) can consider turbulent flow condition. The question whether turbulence in the oncoming flow have a positive or negative effect on bridge flutter cannot be easily answered. Further information about this discussion can be found in Irwin *et al.* (1997).

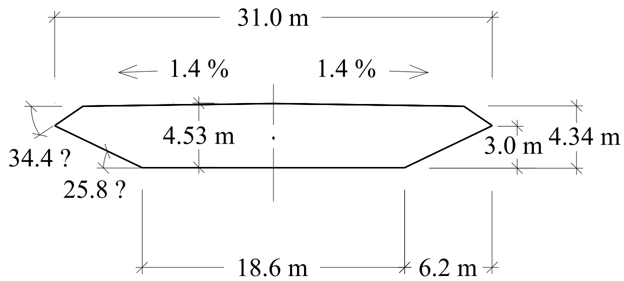

$$m = 17.8 \cdot 10^3 \text{ kg/m}$$
$$I = 2.173 \cdot 10^6 \text{ kgm}$$
$$b = 15.5 \text{ m}$$
$$f_h = 0.099 \text{ Hz}$$
$$f_\alpha = 0.186 \text{ Hz}$$

Fig. 2 Bridge cross section and structural data

4. Example

For the following example, the structural parameters of an erection stage of the Great Belt East Bridge (Walther 1994) were used, see Fig. 2. The structural damping was set to zero. The properties of the ERA system are assumed as follows

$$\begin{aligned} m_c &= 178 \text{ kg/m} \\ e_c &= 2 \text{ m} \end{aligned} \tag{24}$$

The ratio of the total damper mass and the mass of the bridge deck is 2 %. $I_c = 0$ and $b_c = b$ are assumed for simplicity in this initial study. Note, b_c have to be lower than b for installation of the ERA damper completely inside the bridge girder. In Fig. 2, the cross section of the original bridge is shown. The flutter derivatives were determined experimentally using the forced vibration method, cf. Starossek *et al.* (2009). The transformation of frequency-dependent aerodynamic force terms into the time domain is carried out using rational function approximations according to Eq. (18). With two aerodynamic lag terms ($N = 2$), the optimization procedure leads to

$$\begin{aligned} \mathbf{A}_0 &= \begin{pmatrix} -0.0163 & -1.5936 \\ +0.0096 & +0.8012 \end{pmatrix}, \quad \mathbf{D} = \begin{pmatrix} +0.2359 & +0.0652 \\ -0.1097 & +0.0222 \end{pmatrix} \\ \mathbf{A}_1 &= \begin{pmatrix} -0.8322 & -0.7655 \\ +0.5343 & -0.0848 \end{pmatrix}, \quad \mathbf{E} = \begin{pmatrix} -0.5727 & +2.6582 \\ -1.4504 & +1.8480 \end{pmatrix} \end{aligned} \tag{25}$$

$$\mathbf{A}_2 = \begin{pmatrix} -0.6043 & +0.0115 \\ +0.0061 & -0.1005 \end{pmatrix}, \quad \mathbf{R} = \begin{pmatrix} +0.2021 & 0 \\ 0 & +0.5840 \end{pmatrix}$$

The experimentally derived flutter derivatives of the cross section of the Great Belt East Bridge and the results of the rational function approximation are plotted in Fig. 3. For comparison the flutter derivatives for a thin flat plate – analytically determined by Theodorsen, see e.g. Starossek *et al.* (2009) – are presented.

For the bridge structure without ERA, the critical wind speed is $v_{crit}^{uc} = 39.1$ m/s. The numerical simulation scheme for the structure without ERA subjected to aeroelastic forces is not presented here and can be derived omitting the terms of the damper and the equations of γ_1 and γ_2, cf. Eqs. (8) – (11).

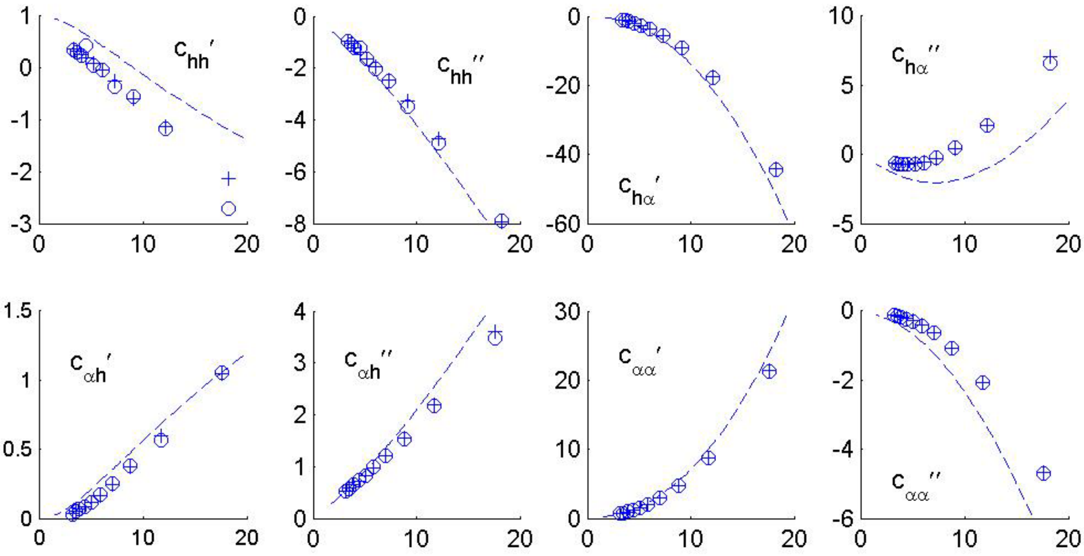

Fig. 3 Flutter derivatives plotted against reduced velocity ($v_{red} = \frac{\pi}{k}$): experimentally determined (o), approximated by rational functions (+), and analytically determined for a thin flat plate ($--$)

Neglecting the aerodynamic forces for control design, a LMI based gain scheduling design is used for the determination of control matrices, cf. Körlin *et al.* (2011). The control matrices are given by

$$\begin{aligned} \mathbf{K}_1 &= (\, 1.8220 \quad 0.3781 \quad -0.5744 \quad -1.2840 \,) \\ \mathbf{K}_2 &= (\, -2.3249 \quad -0.4523 \quad -0.5630 \quad -1.2060 \,) \end{aligned} \tag{26}$$

For the controlled aeroelastic structure, free vibration tests with different initial displacements $\alpha_0 = \alpha(t_0)$ from 0.0035 rad up to 0.1745 rad are numerically simulated. Other displacements disappear at $t = t_0$ in this example. Wind speed υ is increased gradually. If limit cycles are formed in phase portraits, the critical wind speed υ_{crit}^c is found. The critical wind speed of the controlled structure is influenced by the height of the initial displacement as is illustrated by Table 1.

In Section 3.3, the stability performance of the structure equipped with ERA is discussed. For the definition of flutter stability by the results of numerical simulated free vibration tests, an initial displacement has to be chosen. In the view of the authors, this initial displacement is characterized by the performance of the controlled structure in smooth and turbulent flow condition in the range of interesting wind velocities and turbulence intensities. Illustratively, Fig. 4 shows a scenario of the uncontrolled and the controlled structure under turbulent wind condition (Tu = 20 %) with the synchronization of γ_1 and γ_2 and the control forces M_{c1} and M_{c2}, cf. Eq. (7). Compared with the uncontrolled structure, the controlled structure shows reduced amplitudes in the rotational degree of freedom. Assuming for simplicity in this example, however, the rotational displacements can be controlled within the range of $\alpha(t) \leq 0.0349$ rad for the wind speeds and the turbulence intensities of interest, the critical wind speed $\upsilon_{crit}^c = 50.2$ m/s can be found in Table 1. The definition of flutter criterion in the case of significant nonlinearities in the mechanical system of the damper is a topic of future research.

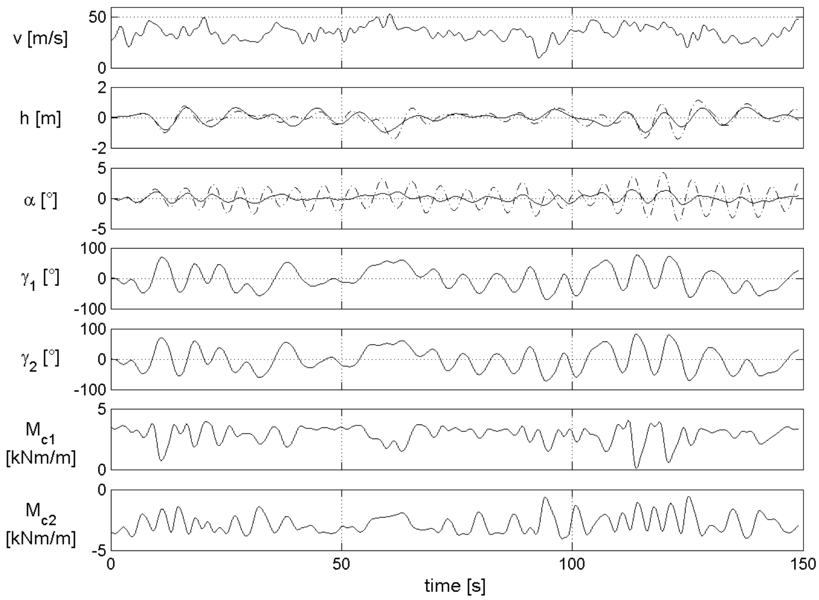

Fig. 4 Scenario in turbulent flow (υ = 35 m/s, Tu = 20 %) of the uncontrolled (· −) and controlled (– –) structure

Table 1 Critical wind speeds $\upsilon_{crit}^c\ (\alpha_0)$

α_0	[rad]	0.0035	0.0175	0.0349	0.0873	0.1745
υ_{crit}^c	[m/s]	53.9	52.6	50.2	43.2	41.8

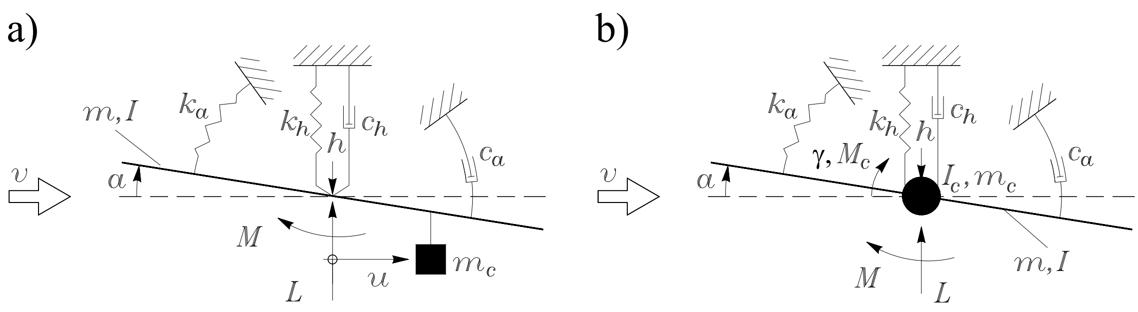

Fig. 5 (a) Movable eccentric mass damper and (b) rotational mass damper

5. Comparison with known active mass dampers for flutter control

In previous studies, two AMDs for flutter control were considered (Körlin and Starossek 2004, 2007). Fig. 5 shows the movable eccentric mass damper (MEMD) and the rotating mass damper (RMD). Because of the coupling of the degrees of freedom h and α by the wind forces, the AMDs are able to dampen not only rotational but also vertical vibrations. According to Körlin and Starossek (2004), the equations of motion of the RMD read

$$\begin{aligned} (m+m_c)\ddot{h} + c_h\dot{h} + k_h h &= -A \\ I\ddot{\alpha} + c_\alpha\dot{\alpha} + k_\alpha\alpha &= M - M_c \end{aligned} \tag{27}$$

with the scalar control force $M_c = I_c\ddot{\gamma}$, i.e. the torque of the centered rotational actuator. The rotational degree of freedom γ is related to the horizontal axis, see Fig. 5. Note that only the control force M_c couples the rotational motion of the damper mass and the rotational degree of freedom of the bridge deck. For comparison study, the control force $u = \ddot{\gamma}$ is used. However, radius of damper mass is set to r_c = 4 m, and $I_c = \frac{1}{2}m_c r_c^2$. With respect to MEMD, the scalar control force is the eccentricity u of the control mass. The linearized equations of motion read as follows

$$\begin{aligned} (m+m_c)\ddot{h} + c_h\dot{h} + k_h h &= -A \\ (I+I_c)\ddot{\alpha} + c_\alpha\dot{\alpha} + k_\alpha\alpha &= M + m_c g u \end{aligned} \tag{28}$$

The numerical simulation of the closed loop performance can be carried out by analogy with the previously introduced procedure (cf. also Körlin and Starossek 2004). For a small-scale model comparison using the given example, several performance criteria shall be analyzed on the basis of control scenarios (time 300 s, v = 35 m/s, and Tu = 1 %, 5 %, or 20 %). Special attention is put to the control's total energy flow over a certain period of time [t_0, t_e]

$$E_c = \int_{t_0}^{t_e} |\, W_c \,|\, \mathrm{d}t \tag{29}$$

where $W_c = I_c \ddot{\gamma}\dot{\gamma}$ ... RMD

$W_c = m_c \ddot{u}\dot{u}$ ... MEMD

$W_c = |M_1\dot{\gamma}_1| + |M_2\dot{\gamma}_2| + \ldots$
$+ m_c g e_c(|\dot{\gamma}_1 \cos\gamma_1| + |\dot{\gamma}_2 \cos\gamma_2|)$ ... ERA.

This quantity is the absolute sum of the mechanical energy which is being fed to the structure plus the mechanical energy which is being extracted. It is assumed that the extracted energy cannot be recovered but must be dissipated (which likewise increase the costs of operation).

The definitions of the performance criteria are shown in Table 2. J_1 is the enhancement of the critical wind speed compared to the uncontrolled structure. Note, the amplitude-dependent critical wind speed of the structure equipped with ERA, see Table 1 and the discussion in section 3.3. J_2 denotes the mass ratio of the active damper. J_3 and J_5 characterize the reduction of the rotational displacement and rotational acceleration of the bridge structure, respectively, where σ denotes the standard deviation. The energy demand of the active damper is J_9 cf. Eq. (29), and the maximum mechanical power is J_{10}. Criteria J_{11}, J_{12}, and J_{13} are the maximum control forces and damper mass displacements. Table 2 shows further the performance criteria of the three dampers, the parameters of which are chosen in such a way that their damping efficiency is approximately equal within the scope of investigated control scenarios, cf. performance criteria J_1, J_2, J_3, and J_5.

Comparing MEMD and RMD, it is shown that RMD has an energy demand of the control that is ten times higher (J_9), whilst the required peak performances are approximately equal (J_{10}). The energy demand and the power requirements of the new damper ERA are smaller by one order of magnitude regarding RMD. This seems to be a decisive advantage for practical implementation of ERA. Fig. 6 shows a practical realization of ERA in a bridge structure. Issues like energy demand, robustness, time delays of real time control implementation, and system reliability are topics of future research. Here, for comparison, and for demonstration of advantages of ERA damper, preliminary design parameters of the numerical simulated dampers RMD and ERA are presented. Because of the generated horizontal forces on the bridge girder by acceleration of damper mass of MEMD, implementation of MEMD is not considered here. For the design of the dampers ERA and RMD, the required control forces are of interest. The maximum control forces, the maximum rotational displacements, and rotation speeds within the simulated control scenarios of RMD and ERA are given in Table 2.

Because of the lumped damper masses are implemented in a spatial, line-like structure of a bridge girder, see Fig. 6, a generalized system is considered. For the preliminary design of the dampers, however, only the one-dimensional generalized system of the torsional mode of the three-dimensional bridge structure is considered. Assuming that the torsional mode is in form of a half-wave sine function, the parameters of the generalized system due to I, I_c, m_c, c_α, and k_α can be derived for the length of the bridge girder of L = 1624 m. For the aerodynamic forces A, and M, and for the control forces M_{c1}, and M_{c2} of ERA and M_c of RMD, the generalization for half-wave sine function is used simplifying. For the mass ratio of μ_c = 2 %, the lumped damper mass m_c of ERA is 144.54 · 10^3 kg. The eccentric arms are driven by electric motors M3BP 400 LKC of ABB

Group with a maximum torque of 3.2 · 4547 Nm and a maximum rotation speed of 1491 rpm. Using a gear reduction of 80:1, the required control moments could be generated by three motors per bridge side. The energy demand of implemented ERA in the numerical simulated control scenario of Tu = 20 % is 5.07 · 10^4 J/m (in 300 s) with a peak performance of 0.18 · 10^4 W/m, cf. Table 2. The required average performance is 0.14 MW, and the required peak performance is 1.5 MW.

The simulated RMD in Table 2 has a lumped damper mass of 289.1 · 10^3 kg. For the maximum control moment M_c = 10.98 kNm/m, respectively 8.92 MNm in generalized system, 16 motors and gear reduction of 40:1 could be used. The required average performance is 2.0 MW, and the required peak performance is 15.7 MW. The power requirements of ERA are an order of magnitude smaller regarding RMD. The implementation effort of ERA is significantly reduced in comparison of RMD.

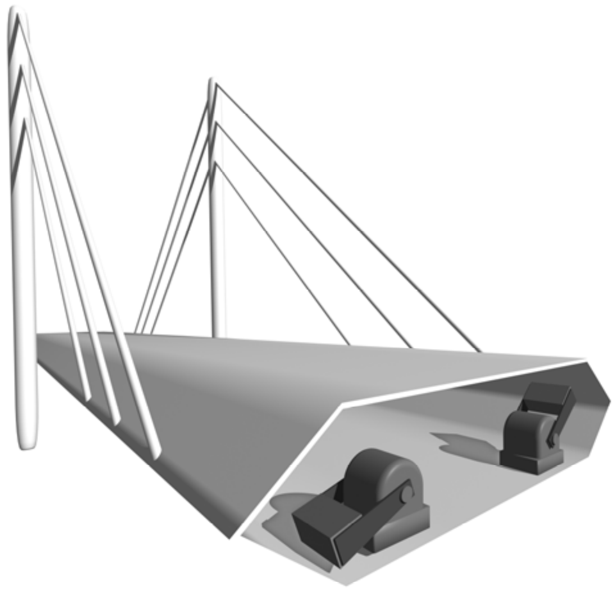

Fig. 6 Preliminary design of ERA in a bridge structure

6. Conclusions

For the control of wind-induced bridge deck vibrations, active mass dampers can be accommodated and can operate completely inside the bridge girder. In this paper, a pair of eccentric rotational actuators (ERA) is used for flutter control of bridges. The equations of motion are established using a bridge girder model that moves in two degrees of freedom and is subjected to wind. In order to take the structural nonlinearities in the ERA system into consideration, a 4th-order Runge-Kutta algorithm is used for numerical simulation of the structural response in the time domain and to carry out the flutter analysis of the controlled system. An example shows the performance of the proposed ERA damper.

Table 2 Performance of active mass dampers for flutter control

Mass damper		MEMD	RMD	ERA
Controller		$u = -7\alpha - 104\dot{\alpha}$	$M_c = 130 I_c \dot{\alpha}$	see Eq. (26)
$J_1 = \frac{v_{crit}^{c} - v_{crit}^{uc}}{v_{crit}^{uc}}$ [%]		27.2	27..2	28.4
$J_2 = \frac{1}{m}\sum \mathrm{m_c}$ [%]		2.0	2.0	2.0
	Tu [%]			
$J_3 = \frac{\sigma_{\alpha,c}}{\sigma_{\alpha,uc}}$ [−]	1	0.37	0.38	0.30
	5	0.37	0.38	0.31
	20	0.25	0.24	0.22
$J_5 = \frac{\sigma_{\ddot{\alpha},c}}{\sigma_{\ddot{\alpha},uc}}$ [−]	1	0.32	0.33	0.23
	5	0.33	0.33	0.24
	20	0.21	0.21	0.17
$J_9 = E_c$ [J/m]	1	$1.75 \cdot 10^2$	$1.78 \cdot 10^3$	$1.25 \cdot 10^2$
	5	$4.27 \cdot 10^3$	$4.37 \cdot 10^4$	$3.06 \cdot 10^3$
	20	$6.93 \cdot 10^4$	$7.21 \cdot 10^5$	$5.07 \cdot 10^4$
$J_{10} = max\lvert W_c \rvert$ [J/(ms)]	1	$0.31 \cdot 10^2$	$0.39 \cdot 10^2$	$0.04 \cdot 10^2$
	5	$0.78 \cdot 10^3$	$0.94 \cdot 10^3$	$0.10 \cdot 10^3$
	20	$1.25 \cdot 10^4$	$1.89 \cdot 10^4$	$0.18 \cdot 10^4$
$J_{11,MEMD} = max\lvert m_c \cdot \ddot{u} \rvert$ [N/m]	1	1750	444	3537
$J_{11,RMD} = max\lvert M_c \rvert$ [Nm/m]	5	7468	2317	3708
$J_{11,ERA} = max\lvert M_{c1,2} \rvert$ [Nm/m]	20	29873	10980	4039
$J_{12,MEMD} = max\lvert \dot{u} \rvert$ [m/s]	1	0.14	0.17	0.07
$J_{12,RMD} = max\lvert \dot{\gamma} \rvert$ [rad/s]	5	0.69	0.82	0.37
$J_{12,ERA} = max\lvert \dot{\gamma}_{1,2} \rvert$ [rad/s]	20	3.00	3.76	1.41
$J_{13,MEMD} = max\lvert u \rvert$ [m]	1	0.13	-	0.14
$J_{13,RMD} = max\lvert \gamma \rvert$ [rad]	5	0.65	-	0.61
$J_{13,ERA} = max\lvert \gamma_{1,2} \rvert$ [rad]	20	3.09	-	1.43

In a small-scale comparison with known active mass dampers for flutter control, the movable eccentric mass damper (MEMD) and the rotational mass damper (RMD), several performance criteria concerning the enhancement of critical wind speed, the mass ratio between damper mass and mass of the bridge girder, the reduction of structural response are used. For MEMD, RMD and ERA, these performance criteria are chosen approximately equal within the scope of investigated control scenarios and the control effort and the energy demand of the systems is investigated and compared. In a case study, a preliminary design of ERA in a bridge structure is presented. The decisive advantage of ERA regarding its technical application lies in a significantly reduced energy demand and the lower implementation effort. Topics of further research are the influence of several parameters of the ERA damper and the investigation of the robustness due to uncertainties in the parameters of the motion-induced aeroelastic forces. Further, the control performance of other devices of interest, e.g., the semi-active dampers and the multiple tuned mass dampers (cf. Abdel-Rohman and Joseph 2006, Gu 2007 and Ubertini 2010), has to be compared weighting the energy demand, the robustness, the safety, and other application issues. So, the technical advantages of the proposed ERA damper can be proved for a realization in a real bridge girder.

Acknowledgements

This research is supported by funds from the Free and Hanseatic City of Hamburg, Germany, under scholarship HmbNFG of the Hamburg University of Technology.

References

Abdel-Rohman, M. and Joseph, M. (2006), "Control of wind-induced nonlinear oscillations in suspension bridges using a semi-active tuned mass damper", *J. Sound Vib.*, **12**(10), 1049-1080.

Bupp, R., Bernstein, D. and Coppola, V. (1995), "A benchmark problem for nonlinear control design: Problem statement, experimental testbed and passive nonlinear compensation", *Proceedings of the American Control Conference*, Seattle, Washington.

Davenport, A. (1962), "Buffeting of a suspension bridge by storm winds", *J. Struct. Div*., **88**(3).

Gu, M. (2007), "Control of wind-induced vibration of long-span bridges and tall buildings", *Front. Struct. Civ. Eng*., **1**(1), 51-62.

Hwang, I., Son, Y., Lee, H., Hong, S., Yoo, D. and Lee, J. (2008), "A damper system for mitigation of suspension bridge flutter", *IABSE, Proceedings of the 17th Congress, Creating and Renewing Urban Structures*, Chicago, IL.

Irwin, P., Xie, J. and Stone, G. (1997), "Controlling factors in the aerodynamic stability of cable stayed bridges", *ASCE, Proceedings of the 15th Structures Congress*, Portland, NY.

Karpel, M. and Strul, E. (1996), "Minimum-state unsteady aerodynamic approximations with flexible constraints", *AIAA, J. Aircraft*, **33**(6), 1190-1196.

Kobayashi, H. and Nagaoka, H. (1992), "Active control of flutter of a suspension bridge", *J. Wind Eng. Ind. Aerod*., **41**(1-3), 143-151.

Körlin, R., Bergmann, D. and Starossek, U. (2004), "Numerical-experimental simulation of active flutter control for bridges", *Struct. Control Hlth*., **11**(2), 141-157.

Körlin, R., Boonto, S., Werner, P. and Starossek, U. (2011), "LMI-based gain scheduling for bridge flutter control using eccentric rotational actuators", *accepted for publication in Optim. Contr. Appl. Met*., .

Körlin, R. and Starossek, U. (2004), "Active mass dampers for flutter control of bridges", *Proceedings of 8th Int. Conf. on Flow-Induced Vibrations*, Paris, France.

Körlin, R. and Starossek, U. (2007), "Wind tunnel test of an active mass damper for bridge decks", *J. Wind Eng. Ind. Aerod*., **95**(4), 267–277.

Kwon, S.D. and Park, K.S. (2003), "Control of Bridge Flutter by TMDs Considering Aerodynamic Uncertainty", *Proceedings of 11th Int. Conf. on Wind Eng*., Lubbock, Texas, USA.

Miyata, T., Yamada, H. and Dung, N. (1996), "Proposed measures for flutter control in long span bridges", *IABSE, Proceedings of the 15th Congress*, Copenhagen, Denmark.

Ostenfeld, K. and Larsen, A. (1992), "Bridge engineering and aerodynamics", *Proceedings of the 1st Int. Conf. on Aerodynamics*, Copenhagen, Denmark.

Phan, D.H. and Kobayshi, H. (2011), "An experimental study of flutter and buffeting control of suspension bridge by mechanically driven flaps", *Wind Struct*., **14**(2), 153-166.

Shinozuka, M. and Jan, C.M. (1972), "Digital simulation of random processes and its application", *J. Sound Vib.*, **25**(1), 111-128.
Simiu, E. and Scanlan, R. (2008), *Wind Effects on Structures: Fundamentals and Application to Design, 3rd edn*, Dover, Mineola, NY, USA.
Spencer Jr., B. and Sain, M. (1997), "Controlling buildings: a new frontier in feedback", *IEEE Control Systems Magazine: Special Issue on Emerging Technologies*, **17**(6), 19-35.
Starossek, U. (1998), "Complex notation in flutter analysis", *ASCE, J. Struct. Eng.*, **124**(8). (Discussion and Closure in **125**(10), 1999).
Starossek, U., Haslan, A. and Thiesemann, L. (2009), "Experimental and numerical identification of flutter derivatives for nine bridge deck sections", *Wind Struct.*, **12**(6), 519-540.
Starossek, U. and Scheller, J. (2008), " novel active mass damper for vibration control of bridges", *Proceedings of 4th Int. Conf. on Bridge Maintenance, Safety, and Management (IABMAS'08)*, Seoul, Korea.
Tiffany, S. and Adams Jr., W. (1987), "Nonlinear programming extensions to Rational Function Aproximation of unsteady aerodynamics", *AIAA Paper 0854*, 406-420.
Ubertini, F. (2010), "Prevention of suspension bridge flutter using multiple tuned mass dampers", *Wind Struct.*, **13**(3), 235-256.
Walther, J.H. (1994), *Discrete Vortex Method for two-dimensional flow past bodies of arbitrary shape undergoing prescribed rotary and translational motion*, PhD thesis, Department of Fluid Mechanics, Technical University of Denmark, Lyngby, Denmark.
Wilde, K., Fujino, Y. and Prabis, V. (1996), "Effects of eccentric mass on flutter of long span bridges", *Proceedings of the 2nd Int. Workshop on Struct. Control*, Hong Kong, China.
Wilde, K., Omenzetter, P. and Fujino, Y. (2001), "Suppression of bridge flutter by active deck-flaps control system", *ASCE, J. Eng. Mech.*, **127**(1), 80-89.

CC